Tanzania Journal of Science 46(2): 290-302, 2020
ISSN 0856-1761, e-ISSN 2507-7961


# Influence of Deposition Temperature on Properties of Multilayered Gallium Doped Zinc Oxide Films Prepared by DC Magnetron Sputtering Technique

**Elisante Maloda[1] and Anayesu B. Malisa[2,*]**
[1]*Department of Physics, Faculty of Science, Dar es Salaam University College of Education, P. O. Box 2329, Dar es Salaam, Tanzania.*
[2]*Department of Physics, College of Natural and Applied Science, University of Dar es Salaam, P. O. Box 35063, Dar es Salaam, Tanzania.*
*E-mail: malodaelisante@yahoo.com; amalisa@udsm.ac.tz*
**Corresponding author*

Received 17 May 2019, Revised 28 April 2020, Accepted 29 April 2020, Published June 2020

**Abstract**

Multilayered transparent conducting films based on ZnO: Ga were deposited onto glass substrate by DC magnetron sputtering technique. The films were prepared from alloy (Zn: Ga) and ceramic (ZnO: Ga) targets with gallium composition of 3 at% and 4 at%, respectively. Crystal structure and phase analysis were measured using X-ray diffractometer (XRD). The XRD structural analysis results indicated that all multilayered films were polycrystalline with (002) orientation slightly shifted of diffracting angles due to gallium dopant concentrations as increase in the deposition temperatures. The films were hexagonal wurtzite structure, having preferred growth orientation in c-axis perpendicular to the substrate surface. The cross section micrographs imaging and elemental composition of multi-layered ZnO: Ga films were studied by Scanning Electron Microscopy (SEM) and Energy Dispersive X-ray spectroscopy (EDX), respectively. The films' surface morphology and grain size approximations were studied by Atomic Force Microscopy (AFM) operated in the tapping mode. Grain size approximations observed in atomic force microscopy scans were confirmed by Debye Scherrer's formula. Optical transmittance and electrical properties of multi-layered films were studied using the UV-VIS spectrophotometer and Ecopia HMS-3000 Hall Effect measurement equipment. Film deposited at substrate temperature of 270 °C showed the best desired results of structural, optical and electrical properties. The film has optical transmittance of over 91% and the lowest resistivity of $1.8 \times 10^{-4}$ Ω-cm corresponding to the highest carrier concentration of $4.8 \times 10^{21}$ $cm^{-3}$ and Hall mobility of 7.5 $cm^2$ /Vs were obtained. The film's band gaps of 3.6 eV and extinction coefficient of 0.43 were computed empirically, while refractive index of 1.75 was calculated by Swanepoel's envelope method from the transmittance spectra. The increase of the films optical band gap arises from among other factors Ga doping concentration and increase of deposition temperatures.

**Keywords:** ZnO: Ga; DC Magnetron Sputtering; Swanepoel's Envelope Method; Thin Films

## Introduction

In recent years, transparent conducting oxides (TCOs) based on zinc oxide (ZnO) thin films have been subjected to numerous investigations and thus have drawn more attention as alternative window materials for solar cells than indium-doped tin oxide (ITO) (Kim and Arifin 2007, Ellimer and Mientus 2008, Yen at el. 2010). The ZnO thin films have wide applications in advanced technology devices such as transparent front contact layer in photovoltaic cells where low resistance and

high transparent window layers are required. It is also widely used in optoelectronic devices like liquid-crystal displays, heat mirrors, light-emitting diodes (LEDs) and laser diodes (LDs) as well as gas sensors (Scott et al. 2011, Gao and Li 2004). The ZnO is a family of group II-VI intrinsic semiconductor materials with a high excitation binding energy of 60 MeV, a wide direct band gap of 3.37 eV at room temperature and a hexagonal wurtzite crystal structure (Xu et al. 2005, Kim et al. 2009). The electro-optical and structural properties of undoped ZnO films are due to native defects like oxygen vacancies ($v_o$) and zinc ion interstitials ($Zn_i$) which increase charge carriers (Wenas et al. 1991, Tahar and Tahar 2005). These defects are not preferable processes to increase charge carriers concentration since they reduce the stability of ZnO films when subjected to higher temperatures. Therefore, it is difficult to control stability of ZnO films by controlling the native defects. The most appropriate technique is the stoichiometric deviation due to impurity doping that creates free electrons as major charge carriers (Park et al. 2009). Impurity doping is achieved by adding foreign elements in the ZnO lattice so as to obtain stable and durable structural as well as high optical and electrical properties of films.

The most preferable possibility is to add trivalent metals such as aluminium, boron, gallium, indium or scandium and yttrium which substitute $Zn^{2+}$ ions in the lattice of ZnO crystal and create free charge carriers in films with stable resistivity for use at high temperatures (Major et al. 1983). Gallium was reported as a promising substitution candidate to the ZnO host lattice. This is because; gallium has less lattice deformation, less reactive and most resistive to oxidation during film formation (Kohiki et al. 1994, Ma et al. 2007). Less lattice deformation is due to the fact that ionic radius of $Ga^{3+}$ (0.62 Å) is much closer to the ionic radius of $Zn^{2+}$ (0.74 Å) compared to that of $Al^{3+}$ (0.54 Å), which makes $Ga^{3+}$ ions to fit into the ZnO lattice more easily than $Al^{3+}$ (Park et al. 2009, Scott et al. 2011). With these reasons, gallium is a promising suitable and potential metallic dopant for transparent conducting window layers for photovoltaic cells. The number of deposition techniques which have been used for the fabrication of ZnO: Ga thin films include metal organic chemical vapour deposition (MOCVD), spray-pyrolysis, pulsed laser deposition (PLD), radio frequency (RF) and direct current (DC) magnetron sputtering.

It was reported that single DC sputtered ZnO: Al and ZnO: Ga window layers have more adverse effects on solar cells than ZnO: B films prepared by MOCVD (Sang et al. 2001). The effect is due to higher-energetic impinging particles on thin film solar cells. However, on one hand, electrical resistivity of ZnO: B films increases with temperature which reduces charge carriers in the conduction band and reducing the performance of films (Sang et al. 2001). Almost resistivity of sputtered ZnO: Ga films do not change with temperature. Electrical resistivity of ZnO: Al films are higher than that of ZnO: Ga films which lowers the optical transmittance and electrical conductivity of the films (Minami et al. 2000, Ma et al. 2007). Thus with these reasons ZnO: Ga films are more stable and can be attributed to the long-term stability and durability for solar cells than those of ZnO: Al and ZnO: B films.

On the other hand, in reducing the adverse effects of high-energetic impinging particles during films deposition, multilayered thin films deposited from Zn: Ga alloy followed by ZnO: Ga ceramic targets provide a possible solution than single layered thin films deposited from ZnO: Ga ceramic target alone (Sang et al. 2001). In this paper, therefore, the influence of deposition temperatures on properties of two single layers of Zn: Ga alloy and ZnO: Ga ceramic targets deposited in that order to obtain a multilayered ZnO: Ga were studied.

## Materials and Methods

### Thin-film deposition

DC reactive magnetron sputtering technique was used to deposit multilayered ZnO: Ga thin films from alloy and ceramic targets, each with a diameter of 5 cm. Gallium compositions in

metallic and ceramic target were 3 at% and 4 at%, respectively with percentage of purity of 99.99%. The films were deposited on ultrasonically cleaned microscopic glass slides/substrates with dimensions of 76 mm x 26 mm x 1 mm. The glass substrate was fixed at a distance of 8.5 cm from the target holder in the sputtering chamber. The films were deposited at different substrate temperatures of 150 °C, 170 °C, 200 °C, 240 °C, 270 °C 300 °C and 330 °C under working other constant deposition parameters like pressure, DC power and argon/oxygen gas ratio flow rate of $6 \times 10^{-3}$ mbar, 75 W and 1.36, respectively. The argon and oxygen gases were used as sputtering and reactive gases, respectively. The targets were pre-sputtered for about 5 minutes while the shutter between the substrate and the target was closed to clean the substrate from contamination and then opened for 25 minutes to allow films deposition. DC reactive magnetron system was based on BALZERS BAE 250 Coating Unit equipped with vane rotary pump and turbo-molecular pump. The vane rotary pump, evacuates the chamber from atmosphere down to pressure below $2.0 \times 10^{-3}$ mbar before switching on the turbo-molecular pump that pumps the chamber down to a pressure in the order of $10^{-6}$ mbar or lower before film deposition. The order of $10^{-6}$ mbar was lowered to the working pressure of the order of $10^{-3}$ mbar by the argon gas.

**Thin-film characterization**

The films thickness was determined by KLR Tencor Alpha-Step 200 profilometer. The structural crystallinity of films were obtained by X-ray diffractometer (XRD, Rigaku RINT III-2000, $CuK_{\alpha}(\lambda = 0.15405$ nm)) instrument operated at 40 kV and 200 mA in a $\theta - 2\theta$ scanning mode. The diffraction angles ( $2\theta$ ) were recorded from 5° to 80° with scanning step and speed of 0.05° and 2°/min, respectively. The cross section micrograph imaging of multilayered ZnO: Ga and elemental compositions of films were obtained using scanning electron microscope (SEM, JEM-7610F, JEOL Ltd., Japan) and energy dispersive X-ray spectroscopy (EDX), respectively. The EDX accelerating voltage during imaging of the samples was in the range of 0 to 10 keV. The EDX (EDS) elemental compositions of the thin film samples were obtained from the equipment output displayed in atomic% and weight%. The atomic%, also expressed as at% is the number of atoms of that element, at that weight percentage, divided by the total number of atoms in the sample multiplied by 100. The weight%, that is the weight percentage of an element, however, is the weight of that element measured in the sample divided by the weight of all elements in the sample multiplied by 100. The multilayered films' surface morphology and grain sizes approximations were obtained using Atomic Force Microscopy (AFM) equipment operated in the tapping mode. Also, the grain sizes were estimated by applying Debye-Scherrer equation (Kim et al. 2009). The optical transmittance data of the multilayered ZnO: Ga thin films were measured using a UV-Vis Spectrophotometer (Perkin Elmer Lambda 950 instrument) in the wavelength ranges of 200 to 800 nm. Below and above this range, the spectra were not obtained. The system is double beam and consists of a light source, sample holder and a photomultiplier tube (PMT) detector for ultraviolet and visible light. Before sample scanning, the background correction was done by inserting bare glass substrate into the holder. Electrical resistivity, carrier concentration and Hall mobility of films were investigated by Ecopia HMS–3000 Hall Effect measurement system using the Van der Pauw method. All measurements were done at room temperature.

**Results and Discussion**

**Structural properties**

The crystal structure and orientation of the multilayered ZnO: Ga thin films deposited at different temperatures were investigated by X-ray diffractometer. The XRD patterns of ZnO: Ga films are shown in Figure 1. All the multilayered films are polycrystalline and have

a hexagonal wurtzite crystal structure. The highest peak intensity corresponding to the (002) peak was observed in all the films. The other orientations (100), (101), (110) and (004) were also observed but with comparatively weak intensities than (002) peak. These peaks are nearly corresponding to those of the theoretical ZnO patterns in JCPDS data file no: 36 1451. The films were grown on preferentially c-axis orientation along the (002) direction, indicating that the growth is perpendicular to substrate plane. The growth of the films in c-axis orientation is due to survival of the fastest nuclei model (Kohiki et al. 1994). The model is explained about as follows: at the initial stage of film growth, the nucleations have various orientations and each nucleus competes to grow but only nuclei having the fastest growth rate can survive. The film peaks (002) appear with diffracting angle slightly shifted to a lower angle than that of the undoped ZnO ( $2\theta$ = 34.45°). On the other hand, diffraction pattern of the films was shifted to large diffraction angle due to the decrease of lattice parameters since the gallium dopant ionic radius is smaller than that of the host zinc (Yen et al. 2010). The small deviation of diffracting angles from undoped Zno indicates that polycrystalline multilayer films have hexagonal wurzite structure similar to that of undoped ZnO but slightly stressed. This implies that the $Zn^{2+}$ in the hexagonal lattice is partially replaced by $Ga^{3+}$ dopant in the films due to increase of deposition temperatures that slightly deteriorates the ZnO lattice along the c-axis (Yen et al. 2010, Ali and Devadason 2011). This may be due to films crystalline improvement as deposition temperatures were increased. Also the crystalline structure of films is due to less lattice deformation of Ga dopant (Janotti and Van de Walle 2009). The less lattice deformation is due to ionic radius of $Ga^{3+}$ (0.62 Å) being much closer to the ionic radius of $Zn^{2+}$ (0.74 Å) which makes $Ga^{3+}$ ions fit into the zinc interstitials.

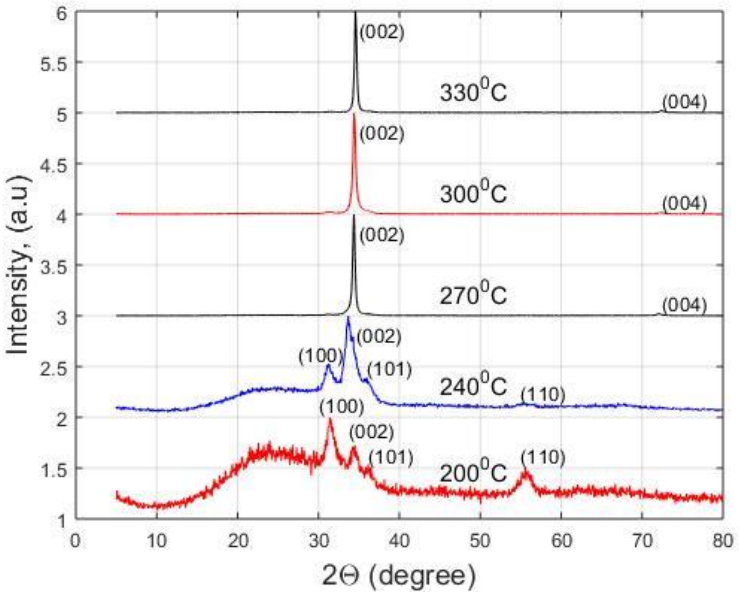


**Figure 1**: The $\theta - 2\theta$ XRD scans of multilayered ZnO: Ga thin films deposited at different substrate temperatures.

The multilayered films lattice constants, a = b and c were calculated using the hexagonal interplanar spacing ($d_{hkl}$) relation given by Equation 1.

$$d_{hkl}^2 = \left[ 4\left( \frac{h^2 + k^2 + hk}{3a^2} \right) + \frac{l^2}{c^2} \right]^{-1} \quad (1)$$

where h, k and l are miller indices. The values of lattice constants a=b and c were calculated from the diffraction peak (002) (Xu et al. 2005). The films lattice constants, full width at half maximum (FWHM) and grains sizes are summarized in Table 1. The calculated lattice constants are nearly corresponding to those of theoretical hexagonal wurtzite crystal structure of ZnO (a = 0.324982 nm and c = 0.520661 nm) (Bhosle et al. 2007). The grain sizes of the films were calculated using Debye-Scherer's formula given by Equation 2.

$$D = \frac{K\lambda}{\beta \cos\theta_{hkl}} \quad (2)$$

where K is the dimensionless constant with the value of 0.9, $D$ is the grain size, $\lambda$ is the X-ray wavelength in nm, $\theta_{hkl}$ is the Bragg diffraction angle and $\beta$ is the full-width at half maximum (FWHM) in radians, however it can also be expressed in degrees. FWHM is the difference between the maximum and minimum of the diffraction angle ($2\theta$) of the full width peak films at the half high peak. All the film grain sizes were evaluated at the diffraction angle and the full width at half maximum of the highest pattern peak (002). The maximum and minimum diffraction angles of the (002) peak in Figure 1 were obtained by extrapolating linear portion of the $2\theta$ at FWHM. Figure 2 shows the cross section micrographs of multilayered ZnO: Ga thin films investigated by SEM. The gallium elemental composition of 0.82 at%, 0.92 at%, 1.09 at%, and 1.41 at%, 1.99 at% in the multilayer films deposited at deferent deposition temperatures were investigated by EDX or EDS technique. The huge variations of gallium elemental compositions in the sample may be due accelerating voltage during EDX scanning which was in the range of 0 to 10 keV. For instance very high accelerating voltages not only decrease spatial resolution but also increase the absorption of x-rays within the sample before they are measured by the detector. Figure 3 depicts atomic force microscopy (AFM) surface morphology scans obtained when the equipment was operated in tapping mode. The films' peak-to-valley distances and grain sizes are approximately 50 nm and less than 50 nm, respectively.

**Table 1:** Influence of deposition temperature (DT) on material properties of multilayered ZnO: Ga thin films

| DT (°C ) | FWHM (°C) | $2\theta$ (°C) (002) | Lattice Constants a (nm) | C (nm) | Grain size (nm) |
|---|---|---|---|---|---|
| 200 | 0.21 | 34.55 | 0.2995 | 0.5188 | 39.57 |
| 240 | 0.18 | 31.55 | 0.3271 | 0.5667 | 45.81 |
| 270 | 0.22 | 33.65 | 0.3071 | 0.5322 | 37.68 |
| 300 | 0.26 | 34.40 | 0.3008 | 0.5210 | 31.95 |
| 330 | 0.25 | 34.40 | 0.3008 | 0.5210 | 33.22 |

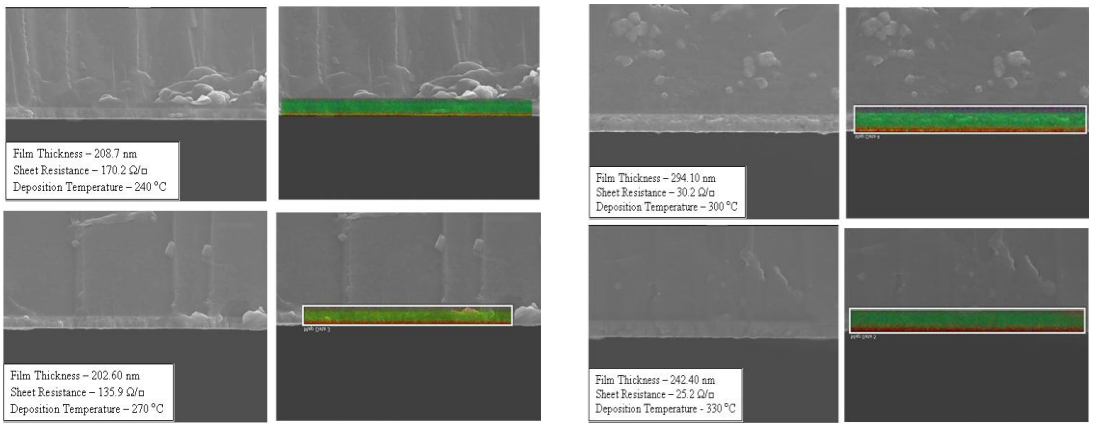


**Figure 2**: SEM and EDX cross section micrographs of multilayered ZnO: Ga deposited at various substrate temperatures.

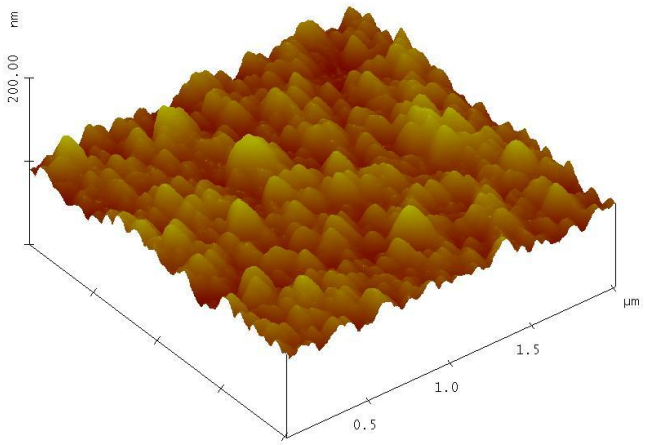


**Figure 3**: AFM representative scan of multilayered ZnO: Ga films deposited at different glass substrate temperatures. The peak-to-valley distance is about 50 nm and grain sizes of the films are approximated to at most 50 nm.

**Optical properties**

Figure 4 shows the transmittance spectra of multilayered ZnO: Ga thin films deposited at different substrate temperatures as a function of wavelengths. The film transmittance was measured at wavelength range of 300 to 800 nm at room temperature. The films exhibit good transmittance above the wavelength of 400 nm as shown in the transmittance spectra. Below the wavelength of 400 nm, a sharp absorption occurs due to the electronic band transition of carriers (Alnajjar 2012). Most of the films except the films deposited at deposition temperature of 330 °C, showed a high transmittance above 80% in the visible region of wavelength range 400 to 700 nm. The

film's low transmittance is due to grain boundaries scattering effects which reflect the light beam. The films deposited at substrate temperatures of 240 °C and 270 °C have the highest transmittance ranging from 89% to 98% and 90% to 93% at the wavelength ranges of 574to 792 nm and 585 to 764 nm, respectively. On the other hand, it was observed that, at temperatures of 150 °C and 300 °C, the highest transmittance lied between 83% and 92%, 81% and 89% in the wavelength ranges of 482 to 690 nm and 488 to 644 nm, respectively. Furthermore, the film transmittance of 86% to 93% at the wavelengths between 651 and 696 nm were obtained at deposition temperatures of 170 °C and 200 °C. The transmittance figure indicates that, film transmittance increased with increasing deposition temperatures from 150 to 270 °C in the wavelength range of 425 to 746 nm. The increase of transmittance is attributed to improvement of film crystalline structure and grain sizes up to the highest appropriate deposition temperature. At the deposition temperatures above 270 °C, the films transmittance decreased as indicated in Figure 4 at the temperature of 330 °C. Therefore, the films deposited at deposition temperatures of 240 °C and 270 °C show the best results of transmittance. This analysis shows that, multilayer films have higher optical transmittance than single layer films as reported in other studies (Song et al. 2002, Nagarani and Sanjeeviraja 2011).

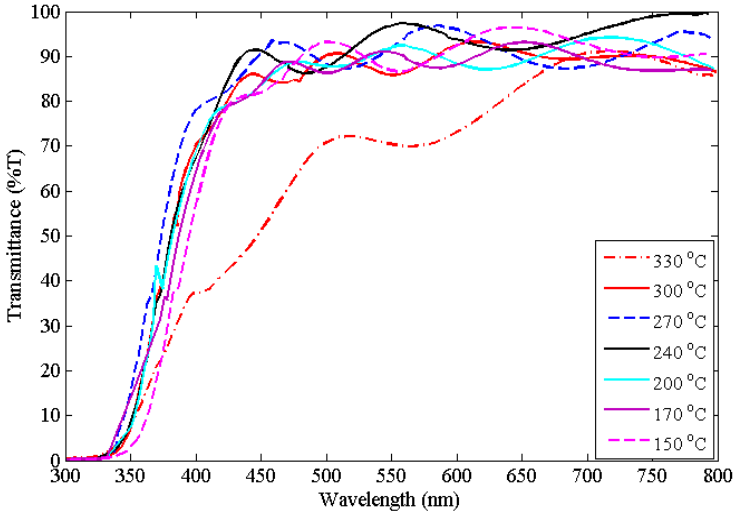


**Figure 4:** Effect of deposition temperature on spectral transmittance of multilayered ZnO: Ga thin films.

Figure 5 presents refractive indices of multilayered ZnO: Ga thin films as a function of wavelengths. Indices were computed empirically using Equation 3 (Shaaban et al. 2012, Caglar et al. 2006, Condurache-Bota et al. 2010).

$$n = \left[ N + \left( N^2 - n_s^2 \right)^{\frac{1}{2}} \right]^{\frac{1}{2}} \qquad (3)$$

where N is a parameter given by Equation 4.

$$N = 2n_s \frac{T_M - T_m}{T_M T_m} + \frac{n_s^2 + 1}{2} \qquad (4)$$

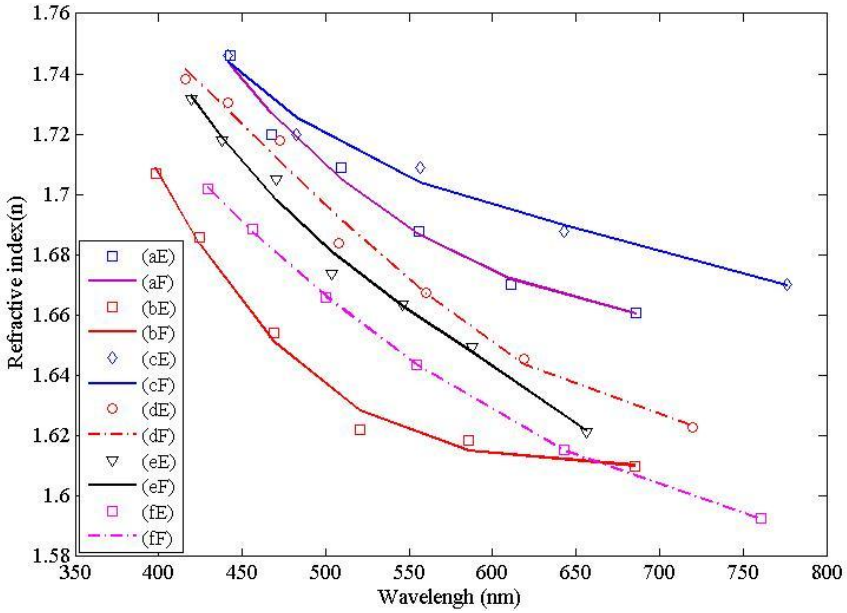


**Figure 5**: Refractive indices of multilayered ZnO: Ga thin films. E represents experimental curves while F represents fitted curves.

Take into account that, the formula is applicable if and only if the regions are of weak and medium absorption. For the transparent region, the N parameter is given by Equation 5.

$$N = \frac{2n_s}{T_m} + \frac{n_s^2 + 1}{2} \qquad (5)$$

The refractive index of the substrate, $n_s$, that is microscope glass slide is calculated from the transmittance data of the substrate alone, $T_s$ which is given by Equation 6.

$$n_s = \frac{1}{T_s} + \left[\frac{1}{T_s^2} - 1\right]^{\frac{1}{2}} \qquad (6)$$

From the theoretical point of view, the values of parameters $T_M$ and $T_m$ (transmission maximum and minimum) were extracted by fitting envelope curves to the upper and lower values of spectrum fringes of Figure 6 and 7. The numbers of $T_{max}$ and $T_{min}$ depend on number of fringes appearing in the spectrum.

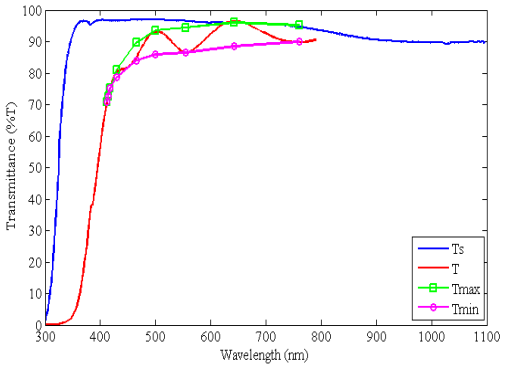


**Figure 6:** Transmittance of multilayered ZnO: Ga deposited at substrate temperature of 240 ˚C including transmittance of bare glass Substrate. $T_{max}$ and $T_{min}$ are the fitted curves of the maximum and minimum of transmittance (T).

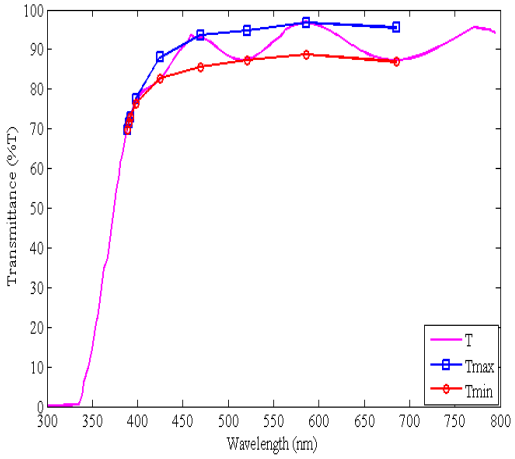


**Figure 7:** Transmittance of multilayered ZnO: Ga thin films deposited at substrate temperature of 270 °C. $T_{max}$ and $T_{min}$ fitted curves of the interference fringes of transmittance (T).

The computed indices of the multilayered ZnO: Ga are in the range of 1.59 to 1.75. The indices of refraction of the films show that, the smaller the refractive index the higher the transmittance and vice versa (Ilican et al. 2007, Condurache-Bota et al. 2010, Shaaban et al. 2012, Gholami et al. 2013 ). Therefore, from Figure 5, the refractive indices of the films represented by (b) and (f) are the best. The films were deposited at substrate temperatures of 270 °C and 240 °C, respectively. Therefore, the refractive index of glass substrate used in the computation of film's refractive index is 1.51.

Extinction coefficients k of multilayered films were calculated using Equation 7 and plotted against wavelengths in Figure 8.

$$k = \frac{\alpha\lambda}{4\pi} \qquad (7)$$

where $\alpha$ is an absorption coefficient given by Equation 8.

$$\alpha = \frac{1}{t} In\left(\frac{1}{T}\right) \qquad (8)$$

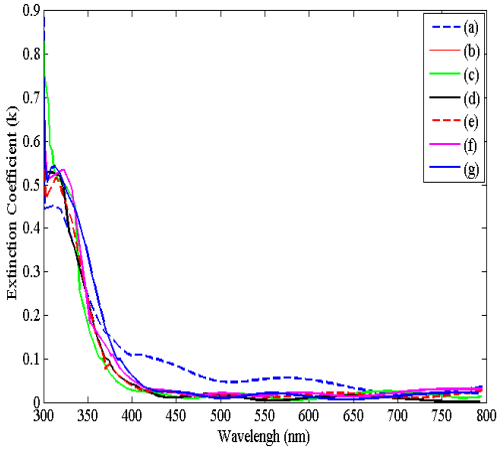


**Figure 8**: Extinction coefficients of multilayered ZnO: Ga thin flims.

The graph shows that the extinction coefficients are large below the wavelength of 400 nm and small above the wavelength of 400 nm. This indicates that at the region of wavelengths below 400 nm light waves are highly absorbed than transmitted and in the region of wavelengths above 400 nm, the light waves are highly transmitted than absorbed. Therefore, the calculated extinction coefficients are confirming theoretical point of view as explained by Ilican et al. (2007) and Condurache-Bota et al. (2010).

It is known that, in ZnO films with high carrier concentrations above the order of $10^{18}$ $cm^{-3}$, the Fermi level lies in the conduction band (Ilican et al. 2007). The increase of carrier concentration influences the absorption edge to shift to shorter wavelengths and hence widening of the optical band gap of films. This historical phenomenon is known as Burstein-Moss (B-M) effect and is shown in Equation 9.

$$E_{opt} = E_{g_o} + \Delta E_g^{BM} \qquad (9)$$

where $E_{g_o}$ is the band gap of the undoped ZnO and $\Delta E_g^{BM}$ is the blue shift of the optical band gap (B-M shift effect). Mathematically, the B-M shift effect is described by Equation 10.

$$\Delta E_g^{BM}(\eta) = \frac{h^2}{8m_{cv}^*}\left(\frac{3\eta}{\pi}\right)^{\frac{2}{3}} \qquad (10)$$

where $m_{cv}^*$ is the reduced effective mass of the valence-conduction band, $\eta$ carrier concentration and other symbols carry their usual meanings. In a direct allowed transition semiconductor, the optical absorption coefficients, $\alpha$ and optical band gaps, $E_{opt}$ are related by Tauc Equation 11.

$$\alpha(h\upsilon) = \beta(h\upsilon - E_{opt})^{\frac{1}{2}} \qquad (11)$$

Where: h is Planck's constant, $\upsilon$ is the frequency of incident photon and $\beta$ is band tailing parameter that depends on the transition probability and is taken as constant within the optical frequency range (Lee et al. 2011). The band gaps of multilayered ZnO: Ga thin films were obtained through plotting $(\alpha h\upsilon)^2$ versus $h\upsilon$ (photon energy) equation as shown in Figure 9. The values of band gaps were obtained by extrapolation technique. Therefore, the plot shows that, the highest value of optical band gap was 3.56 eV which was observed in the films deposited at substrate temperature of 270 °C and the lowest value of 3.30 eV at temperature of 150 °C. The widening of the band gap is due to increase of carrier concentration and deposition temperature increase from 150 to 270 °C.

**Electrical properties**

The electrical resistivity, carrier concentration and mobility of multilayered ZnO: Ga thin films depend strongly on deposition temperature. The Hall Effect Measurement results show that all multilayered ZnO: Ga films are degenerate n-type semiconductors. The films carrier concentrations are in the order of $10^{21}$ $cm^{-3}$ as shown in Table 2 with respect to sheet resistance, resistivity, carrier concentration and hall mobility. The electrical sheet resistance was measured by a 4-point probe (NI PXIe-1062Q).

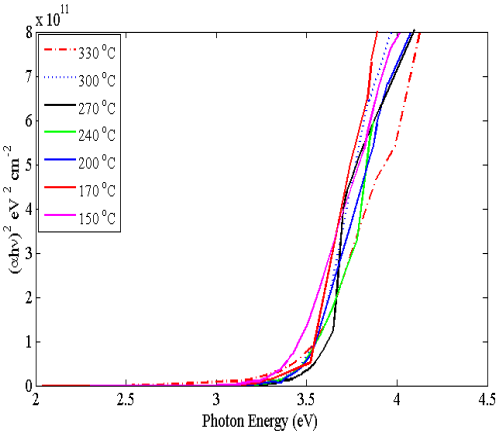


**Figure 9**: $(\alpha h\upsilon)^2$ versus photon energy $(h\upsilon)$ of multilayered ZnO: Ga thin films deposited at different substrate temperatures.

**Table 2:** Variation of deposition temperature (DT) with sheet resistance (SR), resistivity (R), carrier concentration (CC) and Hall Mobility (HM)

| DT (°C) | SR (ohms square) | R (ohms cm x $10^{-4}$) | CC ($cm^{-3}$ x $10^{21}$) | HM ($cm^2$/Vs) |
|---|---|---|---|---|
| 150 | 135.90 | 29.35 | 0.638 | 2.332 |
| 170 | 115.40 | 23.49 | 0.984 | 2.700 |
| 200 | 60.30 | 20.12 | 0.699 | 4.439 |
| 240 | 25.20 | 2.670 | 2.612 | 8.953 |
| 270 | 20.80 | 1.794 | 4.756 | 7.830 |
| 300 | 30.20 | 2.507 | 4.620 | 5.025 |
| 330 | 42.20 | 11.79 | 1.457 | 3.635 |

Figure 10 represents the variations of electrical resistivity, carrier concentrations and mobility as a function of deposition temperature. It is observed that, as deposition temperature increased from 150 to 270 °C, the films resistivity decreased while carrier concentrations and mobility gradually increased. This is due to the improvement in the films crystallinity and a decrease of grain boundary scattering in the films as deposition temperature increased. The grain boundary scatterings act as barriers of free carriers'

migration (Yang et al. 2013, Nagarani and Sanjeeviraja 2011). At the maximum point, carrier concentrations, Hall mobility and resistivity decreased. The results show that, the lowest resistivity of $1.8 \times 10^{-4}\ \Omega - cm$ corresponding to the highest carrier concentration of $4.8 \times 10^{21}$ $cm^{-3}$ was obtained at substrate temperature of 270 °C. Moreover, at deposition temperature of 240 °C, the highest mobility of 9.0 $cm^2/Vs$ was obtained. At temperatures above 270 °C, the films resistivity increased up to $1.2 \times 10^{-3}\ \Omega - cm$ at a temperature of 330 °C, while the carrier concentrations and mobility decreased. The increase of resistivity and decrease of mobility are due to ionized impurity scattering which act as a barrier of carriers movement. The decrease of films resistivity and increase of mobility and carrier concentration can also be explained in terms of films crystallinity and grain sizes (Bhosle et al. 2007).

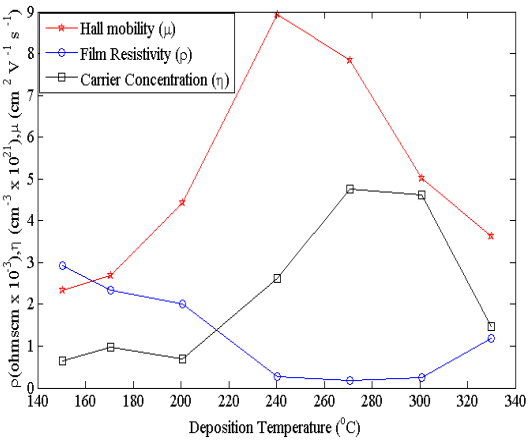


**Figure 10:** The electrical resistivity, carrier concentration and Hall Mobility of multilayered ZnO: Ga as a function of deposition temperature.

## Conclusion

The multilayered ZnO: Ga films were prepared from alloy and ceramic targets with gallium content of 3 at% and 4 at%, respectively. Gallium element compositions in the multilayered films were found using EDX to be in the range of 0.82 at% to 1.99 at% with an average of 1.246 at%. The targets were sputtered by DC magnetron sputtering technique. All multilayered films were polycrystalline having a preferred growth orientation in the c-axis perpendicular to the substrate plane and dominant diffraction peak of (002). The best results were obtained for a film deposited at substrate temperature of 270 °C. The highest optical transmittance of over 91%was obtained at wavelength of about 574 nm. The film had a band gap of 3.56 eV. The computed refractive indices and extinction coefficients are small at high transmittance and large at low transmittance as depicted in Figure 5 and 8, respectively. The obtained refractive indices and extinction coefficients were in the range of 1.59 to 1.75 and 0.02 to 0.75, respectively. The lowest resistivity of $1.794 \times 10^{-4}\ \Omega cm$ , corresponding with the highest carrier concentration of $4.756 \times 10^{21}$ $cm^{-3}$ and a Hall Mobility of 7.530 $cm^2/Vs$ as depicted in Figure 10 were obtained.

## Acknowledgment

The authors acknowledge assistance from the Basic Science Research Program through the National Research Foundation of Korea (NRF), as funded by the Korean Government (2013K1A3A1A09075971) for the structural characterization of the samples. Special thanks go to Dar es Salaam University College of Education (DUCE) under the Science and Technology Higher Education Program (STHEP) of the World Bank project for financial support. The authors also acknowledge the Government Chemist Laboratory Authority (GCLA) of Tanzania for optical measurement assistance, and lastly the Solar Energy Research Group of the Department of Physics, University of Dar es Salaam for laboratory access while doing sample preparations and electrical measurements of the samples.

## References

Ali FA and Devadason S 2011 Growth and characterization of cerium doped zinc oxide

nanocrystalline thin film. *Journal of Pure Appl. Indust. Phys* 1(2): 115-120.

Alnajjar AA 2012 ZnO: Al grown by sputtering from two different target sources: a comparison study. *Adv. Condens. Matter Phys.* 2012 Article ID 682125, 8 p.

Bhosle V, Prater JT, Yang F, Burk D, Forrest SR and Narayan J 2007 Gallium-doped zinc oxide films as transparent electrodes for organic solar cell applications. *J. Appl. Phys.* 102: 23501-23505.

Caglar M, Caglay Y and Ilican S 2006 The determination of the thickness and optical constants of the ZnO crysalline thin film by using envelope method. *J. Optoelectron. Adv. Mater.* 8(4): 1410-1413.

Condurache-Bota S, Tigau N and Drasovean R 2010 Explicit application of Swanepoel's method for the analysis of $Sb_2O_3$ films. *J. Sci. Arts* 2(13): 335-340.

Ellimer K and Mientus R 2008 Carrier transport in polycrystalline transparent conductive oxides: A comparative study of zinc oxide and indium oxide. *Thin solid Films* 516: 4620-4627.

Gao W and Li Z 2004 ZnO thin films produced by magnetron sputtering. *Ceram. Int.l* 30 (7): 1155-1159.

Gholami M, Nazari A, Azarin K, Yazdanimeher S and Sadeghaniya B 2013 Determination of the thickness and optical constants of metal oxide thin films by different methods. *J. Basic Appl. Sci. Res.* 3: 597-600.

Ilican S, Caglar, M and Caglar Y 2007 Determination of the thickness and optical constant of transparent indium-doped ZnO thin films by envelope method. *Materials Science–Poland* 25(3): 709–718.

Janotti A and Van de Walle CG 2009 Fundamentals of zinc oxide as a Semiconductor: *Rep. Progr. Phys.* 72 (12): 126501.

Kim G, Bang J, Kim Y, Rout SK and Woo SI 2009 Structural, electrical and optical properties of boron doped ZnO thin films using LSMCD method at room temperature. *Appl. Phys. A. Mater Sci. Proces.* 97(4): 821-828.

Kim HK and Arifin E 2007 The effect of gallium concentration and substrate temperature on the properties of Ga–doped ZnO thin films sputtered from powder compacted target. *Metal Mater. Int.* 13(6): 489-494.

Kohiki S, Nishitani M and Wada T 1994 Enhanced electrical conductivity of zinc oxide thin films by ion implantation of gallium, aluminium and boron atoms. *J. Appl. Phys.* 75(4): 2069-2072.

Lee S, Cheon D, Kim WJ, Ahn KJ and Lee W 2011 Combined effect of the target composition and deposition temperature on the properties of ZnO:Ga transparent conductive oxide films in pulsed DC magnetron sputtering. *Semiconduct. Sci. Technol.* 26(11): p. 115007.

Ma Q, Ye Z, He H, Zhu L, Wang J and Zhao B 2007 Influence of $Ar/O_2$ ratio on the properties of transparent conductive ZnO: Ga films prepared by DC reactive magnetron sputtering. *Materials Letters* 61: 2460-2463.

Major S, Chopra KL and Pandya DK 1983 Transparent conductors. a status review. *Thin Solid Films* 102(1): 1-46.

Minami T, Yamamoto T and Miyata T 2000 Highly transparent and conductive rare earth-doped ZnO thin films prepared by magnetron sputtering. *Thin Solid Films* 366(1-2): 63-68.

Nagarani S and Sanjeeviraja C 2011 Structural, electrical and optical properties of gallium doped ZnO: Ga thin films prepared by electron beam evaporation technique. *Am. Inst. Phys., Conf. Proc* 1349(1): 589-590, American Institute of Physics.

Park SE, Lee JC, Song PK and Lee JH 2009 Properties of gallium-doped zinc-oxide films deposited by RF or DC magnetron sputtering with various GZO targets. *J. Korean Phys. Soc*. 54: 1283-1287.

Sang B, Kushiya K, Okumura D and Yamase O 2001 Performance improvement of CIGS-based modules by depositing high-quality

Ga-doped ZnO windows with magnetron sputtering. *Solar Energy Mater. Solar Cells* 67(1-4): 237-245.

Scott RC, Leedy KD, Bayraktaroglu B, Look DC, Smith DJ, Ding D, Lu X and Zhang Y 2011 Influence of substrate temperature and post-deposition annealing on material properties of Ga-doped ZnO prepared by pulsed laser deposition. *J. Electron. Mater*: 40(4): 419-428.

Shaaban ER, Yahia IS and El–Metwally EG 2012 Validity of Swanepoel's method for calculating the optical constants of thick films. *Acta Phys. Pol. A* 121(3): 628-635.

Song PK, Watanabe M, Kon M, Mitsui A and Shigesato Y 2002 Electrical and optical properties of gallium-doped zinc oxide films deposited by DC magnetron sputtering. *Thin Solid Films* 411 (1): 82-86.

Tahar RBH and Tahar NBH 2005 Boron doped zinc oxide thin films prepared by sol-gel technique. *J. Mater. Sci.* 40(19): 5285-5289.

Wenas WW, Yamada A, Takahashi K, Yoshino M and Konagai M 1991 Electrical and optical properties of boron doped ZnO thin films for solar cells grown by metalorganic chemical vapour deposition. *J. Appl. Phys.* 70(11): 7119-7123.

Xu HY, Liu YC, Mu R, Shao CL, Lu YM, Shen DZF and Fan XW 2005 F-doping effects on electrical and optical properties of ZnO nanocrystalline films. *Appl. Phys Lett.* 86(12): p.123107.

Yang WF, Liu ZG, Wu ZY, Hong MH, Wang CF, Lee AYS and Gong H 2013 Low substrate temperature fabrication of high-performance metal oxide thin film by magnetron sputtering with target self-heating. *Appl. Phys. Lett.* 102: p.111901.

Yen WT, Lin YC, Yao PC, Ke JH and Chen YL 2010 Growth characteristics and properties of ZnO: Ga thin films prepared by pulsed DC magnetron sputtering. *Appl. Surf. Sci.* 256(11): 3432-3437.